Neuropsychopharmacology

ARTICLE

(2*R*,6*R*)-hydroxynorketamine rapidly potentiates hippocampal glutamatergic transmission through a synapse-specific presynaptic mechanism

Lace M. Riggs[1,2], Yasco Aracava[3], Panos Zanos[2], Jonathan Fischell[4], Edson X. Albuquerque[3,5], Edna F. R. Pereira[3,5], Scott M. Thompson[2,4] and Todd D. Gould[2,5,6,7]

Preclinical studies indicate that (*2R,6R*)-hydroxynorketamine (HNK) retains the rapid and sustained antidepressant-like actions of ketamine, but is spared its dissociative-like properties and abuse potential. While (*2R,6R*)-HNK is thought to exert its antidepressant-like effects by potentiating α-amino-3-hydroxy-5-methyl-4-isoxazolepropionic acid receptor (AMPAR)-mediated synaptic transmission, it is unknown how it exerts this effect. The acute synaptic effects of (*2R,6R*)-HNK were examined by recording field excitatory postsynaptic potentials (fEPSPs) and miniature excitatory postsynaptic currents (mEPSCs) in rat hippocampal slices. (*2R,6R*)-HNK bath application caused a rapid and persistent potentiation of AMPAR-mediated Schaffer collateral (SC)-CA1 fEPSPs in slices derived from male and female rats. The (*2R,6R*)-HNK-induced potentiation occurred independent of *N*-methyl-D-aspartate receptor (NMDAR) activity, was accompanied by a concentration-dependent decrease in paired pulse ratios, and was occluded by raising glutamate release probability. In additon, in the presence of tetrodotoxin, (*2R,6R*)-HNK increased the frequency, but not amplitude, of mEPSC events, confirming a presynaptic site of action that is independent of glutamatergic network disinhibition. A dual extracellular recording configuration revealed that the presynaptic effects of (*2R,6R*)-HNK were synapse-selective, occurring in CA1-projecting SC terminals, but not in CA1-projecting temporoammonic terminals. Overall, we found that (*2R,6R*)-HNK enhances excitatory synaptic transmission in the hippocampus through a concentration-dependent, NMDAR-independent, and synapse-selective increase in glutamate release probability with no direct actions on AMPAR function. These findings provide novel insight regarding (*2R,6R*)-HNK's acute mechanism of action, and may inform novel antidepressant drug mechanisms that could yield superior efficacy, safety, and tolerability.

Neuropsychopharmacology (2020) 45:426–436; https://doi.org/10.1038/s41386-019-0443-3

INTRODUCTION

Depression claims the highest burden of disease among neuropsychiatric disorders and is one of the leading causes of disability worldwide [1]. Monoamine-based antidepressant treatments have prevailed for almost 70 years, despite their slow therapeutic onset and failure to provide complete or permanent remission to most patients [2]. An important advancement for the treatment of depression was the discovery that (*R,S*)-ketamine (*ketamine*) could rapidly alleviate symptoms of depression within hours of a single subanesthetic dose administration [3, 4]. In addition to its rapid antidepressant properties, ketamine is reported to rapidly mitigate symptoms of post-traumatic stress disorder [5], suicidality [6–8], obsessive compulsive disorder [9, 10], and anhedonia [11, 12]. The rapid onset with which ketamine exerts these broad therapeutic effects makes its discovery one of the most significant advances in psychiatry in recent decades. However, the use of ketamine to treat psychiatric indications is limited by the dissociative properties [13, 14] and abuse potential [15] that are conferred, at least in part, by its actions as an *N*-methyl-D-aspartate receptor (NMDAR) antagonist [16].

Ketamine is thought to exert its antidepressant effects though a rapid change in neuronal function, which then gives rise to persistent changes that last from days-to-weeks after ketamine has been eliminated from the body. Considerable effort has been made to understand the nature of these changes [17, 18]. Dominant hypotheses focus on acute NMDAR inhibition by ketamine, either at NMDARs localized to γ-aminobutyric acid (GABA)-ergic inhibitory interneurons [19–21], extrasynaptic GluN2B-containing NMDARs [22], or synaptic NMDARs at rest [23, 24]. However, despite these theoretical advancements in understanding the synaptic effects of NMDAR inhibition *vis-à-vis* ketamine, alternative NMDAR antagonists have largely failed to exert the full spectrum of ketamine's antidepressant effects in clinical trials [25].

[1]Program in Neuroscience, University of Maryland School of Medicine, Baltimore, MD 21201, USA; [2]Department of Psychiatry, University of Maryland School of Medicine, Baltimore, MD 21201, USA; [3]Department of Epidemiology and Public Health, Division of Translational Toxicology, University of Maryland School of Medicine, Baltimore, MD 21201, USA; [4]Department of Physiology, University of Maryland School of Medicine, Baltimore, MD 21201, USA; [5]Department of Pharmacology, University of Maryland School of Medicine, Baltimore, MD 21201, USA; [6]Department of Anatomy and Neurobiology, University of Maryland School of Medicine, Baltimore, MD 21201, USA and [7]Veterans Affairs Maryland Health Care System, Baltimore, MD 21201, USA
Correspondence: Todd D. Gould (gouldlab@me.com)
Senior authors: Scott M. Thompson and Todd D. Gould.

Received: 6 March 2019 Revised: 17 May 2019 Accepted: 11 June 2019
Published online: 19 June 2019

Existing literature suggests that alternative mechanisms can be engaged by compounds that have rapid antidepressant potential, which act to restore the balance between excitation and inhibition throughout the mesocorticolimbic system, known to be disrupted in depression [18, 26–28]. Similar to both ketamine [29] and non-NMDAR-antagonists with rapid antidepressant potential [18], α-amino-3-hydroxy-5-methyl-4-isoxazolepropionic acid receptor (AMPAR) activation is required for the rapid antidepressant-like effects of the ketamine metabolite, (2R,6R)-hydroxynorketamine (HNK). (2R,6R)-HNK has shown rapid and sustained antidepressant-relevant behavioral and cellular actions [30–39], but is spared many of ketamine's adverse effects [30, 39] given its low potency to inhibit NMDAR function relative to ketamine [30, 40–42]. While (2R,6R)-HNK acutely potentiates AMPAR-mediated synaptic transmission in the hippocampus [30], it is unknown how it exerts these effects. In the current study, we show that (2R,6R)-HNK selectively enhances excitatory synaptic transmission in the hippocampus through a concentration-dependent increase in glutamate release probability. Notably, our results indicate that (2R,6R)-HNK leads to a presynaptic potentiation that does not require NMDAR activation, is not occluded by NMDAR inhibition, and that persists in the presence of tetrodotoxin (TTX), thus excluding GABAergic network disinhibition as being necessary for these effects. These findings provide a foundation for future studies to identify the specific mechanism by which (2R,6R)-HNK exerts its effects, and will promote the development of novel antidepressant compounds that may possess superior efficacy, safety, and tolerability than those currently available.

MATERIALS AND METHODS

See Supplemental Materials and Methods for complete details.

Animals

For extracellular slice electrophysiology, male and female Sprague Dawley rats (postnatal day [PD] 28 on arrival; Charles River, MA) were acclimated to the vivarium (University of Maryland, Baltimore, MD) for at least 1 week prior to experiments. For whole-cell slice electrophysiology, male Sprague Dawley rats (PD8 on arrival; Charles River, MA) were acclimated to the vivarium with a nursing dam until weaning (PD21), and experiments occurred at PD25-35. All rats were housed three per cage under standard conditions (12-h light-dark cycle) with food and water available *ad libitum*. All experimental procedures were approved by the University of Maryland Baltimore Animal Care and Use Committee and were conducted in full accordance with the National Institutes of Health Guide for the Care and Use of Laboratory Animals.

Extracellular slice electrophysiology

Standard methods were used to prepare transverse hippocampal slices (400-µm thickness). Dissecting and recording artificial cerebrospinal fluid (ACSF) contained (in mM): 120 NaCl, 3 KCl, 1 NaH_2PO_4, 25 $NaHCO_3$, 1.5 $MgSO_4{\cdot}7H_2O$, 2.5 $CaCl_2$, and 20 glucose, and was carbogenated with 95% O_2/5% CO_2. Nominally free Mg^{2+} recording ACSF contained (in mM): 120 NaCl, 3 KCl, 1 NaH_2PO_4, 25 $NaHCO_3$, 2.5 $CaCl_2$, and 20 glucose, and was carbogenated with 95% O_2/5% CO_2.

Whole-cell slice electrophysiology

The whole-cell patch-clamp technique was used to record miniature excitatory postsynaptic currents (mEPSCs) from the soma of CA1 pyramidal neurons voltage clamped at −60 mV in the presence of bath applied TTX. Standard procedures were used to prepare transverse hippocampal slices (300-µm thickness). Dissecting ACSF contained (in mM): 125 NaCl, 2.5 KCl, 1.25 NaH_2PO_4, 26 $NaHCO_3$, 1 $MgCl_2$, 2 $CaCl_2$, and 25 glucose, and was carbogenated with 95% O_2/5% CO_2.

Chemicals

(2R,6R)-HNK was synthesized at the National Center for Advancing Translational Sciences (Bethesda, MD), and absolute and relative stereochemistry were confirmed by small molecule x-ray crystallography [30, 43]. All compounds were diluted to their final concentration in ACSF.

Experimental design and statistical analysis

All experiments were performed in a randomized fashion and conducted and analyzed by experimenters blind to the treatment. Data were analyzed with GraphPad Prism Software 7.04, with statistical significance defined as $p < 0.05$.

RESULTS

(2R,6R)-HNK causes an NMDAR-independent enhancement of AMPAR-mediated synaptic transmission in hippocampal slices from male and female rats

Hippocampal slices from male and female rats were superfused with (2R,6R)-HNK (10 µM) for 1 h. In hippocampal slices from male rats (Fig. 1a), (2R,6R)-HNK significantly increased the slope of Schaffer collateral (SC)-CA1 field excitatory postsynaptic potentials (fEPSPs) to 162 ± 14% of baseline (Fig. 1b, c; $t_{(5)} = 4.424$, $p = 0.0069$, $n = 6$), without changing fiber volley (FV) amplitude (Fig. 1b). The effect of (2R,6R)-HNK did not reverse following a 30-min washout with (2R,6R)-HNK-free ACSF (158 ± 12%; Fig. 1b). We observed similar results with the use of hippocampal slices from females (Fig. 1d), in which (2R,6R)-HNK led to a 157 ± 14% potentiation of SC-CA1 fEPSPs (Fig. 1e, f; $t_{(5)} = 4.018$, $p = 0.0101$, $n = 6$); this effect also persisted during washout (166 ± 19%). In both cases, fEPSPs were blocked by superfusion of the slices with 6,7-dinitroquinoxaline-2,3(1H,4H)-dione (DNQX, 50 µM)-containing ACSF (Fig. 1b, e), indicating that the synaptic potentials were mediated by AMPARs under these recording conditions. There was no significant difference between results obtained from male- and female-derived slices at the (2R,6R)-HNK concentration tested ($t_{(11)} = 0.1511$, $p = 0.8826$), suggesting that intrinsic organizational sex differences do not modulate the potentiation induced by (2R,6R)-HNK. We note that rats were of prepubertal age and therefore activational effects of fluctuating hormones are not implicated in our findings. Thus, all subsequent experiments were conducted in hippocampal slices derived from male rats.

To determine whether NMDAR activity modulated the potentiating effects of (2R,6R)-HNK, experiments were performed in hippocampal slices continuously superfused with ACSF containing the competitive NMDAR antagonist, 2-amino-5-phosphonopentanoic acid (AP5, 80 µM; Fig. 1g). (2R,6R)-HNK potentiated SC-CA1 fEPSPs to 153 ± 13% of baseline in the presence of AP5 (Fig. 1h, i; $t_{(6)} = 3.928$, $p = 0.0077$, $n = 7$), indicating that the acute enhancement in AMPAR-mediated synaptic transmission is NMDAR-activity-independent.

(2R,6R)-HNK exerts its acute synaptic effects through a concentration-dependent increase in the probability of glutamate release

Slices were bathed with various concentrations of (2R,6R)-HNK (0.3, 1, 3, 10, 30 µM; Fig. 2a) revealing that the (2R,6R)-HNK-induced potentiation of SC-CA1 fEPSPs was concentration-dependent (Fig. 2b). (2R,6R)-HNK had no effect on FV amplitude, regardless of concentration (Fig. 2c). When comparing each concentration to its baseline (Fig. 2e), (2R,6R)-HNK induced a significant potentiation at 3 µM ($t_{(6)} = 3.465$, $p = 0.0134$, $n = 7$), 10 µM ($t_{(6)} = 5.981$, $p = 0.0010$, $n = 7$), and 30 µM ($t_{(6)} = 3.985$, $p = 0.0072$, $n = 7$). Such potentiation was not observed in slices superfused with vehicle (VEH; $t_{(3)} = 1.565$, $p = 0.2155$, $n = 4$) or (2R,6R)-HNK at 0.3 µM ($t_{(4)} = 0.2314$, $p = 0.8284$, $n = 5$) or 1 µM ($t_{(7)} = 1.237$, $p = 0.2561$, $n = 8$). Between-group comparisons revealed a significant main effect of (2R,6R)-HNK on the change

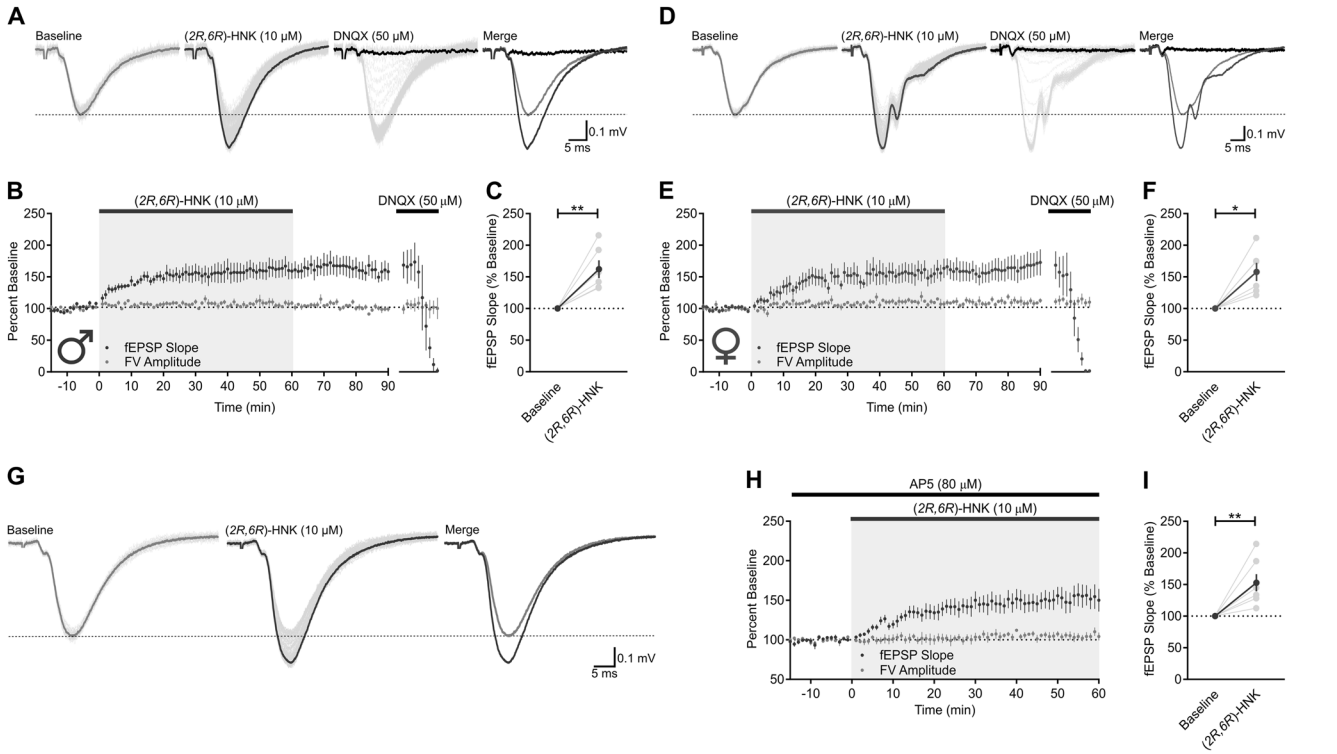

Fig. 1 *(2R,6R)-HNK causes an NMDAR-independent enhancement of AMPAR-mediated synaptic transmission in hippocampal slices from male and female rats*. Representative traces of Schaffer collateral (SC)-CA1 field excitatory postsynaptic potentials (fEPSPs) recorded from **a** male and **d** female Sprague Dawley rats. Individual sweeps across the procedure (light gray) are overlaid with terminal averages during baseline (gray), (2*R*,6*R*)-hydroxynorketamine (HNK) superfusion (blue), and 6,7-dinitroquinoxaline-2,3(1H,4H)-dione (DNQX) superfusion (black). **b** Bath application of (2*R*,6*R*)-HNK (10 μM) to male ($n = 6$) and **e** female ($n = 6$) hippocampal slices enhanced the slope of SC-CA1 fEPSPs, which were mediated by α-amino-3-hydroxy-5-methyl-4-isoxazolepropionic acid receptor (AMPARs), given that they were blocked by DNQX (50 μM). The (2*R*,6*R*)-HNK-induced potentiation of fEPSPs persisted in (2*R*,6*R*)-HNK-free artificial cerebrospinal fluid (ACSF), and did not influence presynaptic fiber volley (FV) amplitude. fEPSP slope was significantly higher during the last 10 min of (2*R*,6*R*)-HNK superfusion of **c** male and **f** female slices when compared to baseline. **g** Representative traces of SC-CA1 fEPSPs recorded from male Sprague Dawley rats in the presence of 2-amino-5-phosphonopentanoic acid (AP5, 80 μM). Individual sweeps across the procedure (light gray) are overlaid with terminal averages during baseline (gray) and after (2*R*,6*R*)-HNK superfusion (blue). **h** (2*R*,6*R*)-HNK superfusion enhanced the slope of SC-CA1 fEPSPs in the presence of AP5 ($n = 7$). **i** fEPSP slope was significantly higher during the last 10 min of (2*R*,6*R*)-HNK superfusion when compared to baseline. *$p < 0.05$, **$p < 0.01$. Points and error bars represent mean and standard error of the mean, respectively

in SC-CA1 fEPSPs (Fig. 2f; $F_{(5,32)} = 8.299$, $p < 0.0001$), with the fEPSP slopes being significantly larger in the presence of 10 μM than VEH ($p = 0.0075$) or (2*R*,6*R*)-HNK at 0.3 μM ($p = 0.0024$) and 1 μM ($p = 0.0029$). Likewise, fEPSP slopes were larger in the presence of 30 μM (2*R*,6*R*)-HNK than VEH ($p = 0.0065$) or (2*R*,6*R*)-HNK at 0.3 μM ($p = 0.0020$) and 1 μM ($p = 0.0024$). Analysis of the concentration-response relationship generated by plotting the change in fEPSP slope as a function of (2*R*,6*R*)-HNK concentration revealed an EC_{50} of 3.3 μM (Fig. 2g).

We next asked whether changes in presynaptic release probability could account for this potentiation by measuring paired pulse ratios (PPRs) before and after (2*R*,6*R*)-HNK superfusion. (2*R*,6*R*)-HNK-induced increases in fEPSP slope significantly correlated with changes in PPR (Fig. 2d; $R^2 = 0.2784$, $p = 0.0007$), indicating that the degree of change in glutamate release probability significantly predicts the magnitude of the potentiation induced by (2*R*,6*R*)-HNK. When compared to baseline (Fig. 2h), (2*R*,6*R*)-HNK led to a significant reduction in PPR at 3 μM ($t_{(6)} = 3.57$, $p = 0.0118$), 10 μM ($t_{(6)} = 2.994$, $p = 0.0242$), and 30 μM ($t_{(6)} = 6.677$, $p = 0.0005$), but not under VEH ($t_{(3)} = 0.69$, $p = 0.5398$), 0.3 μM ($t_{(4)} = 1.101$, $p = 0.3328$), or 1 μM ($t_{(7)} = 2.063$, $p = 0.0780$) conditions. When comparing among concentrations, there was a significant main effect of (2*R*,6*R*)-HNK on the PPR change (Fig. 2i; $F_{(5,32)} = 4.007$, $p = 0.0062$), with the change observed in slices superfused with (2*R*,6*R*)-HNK at 10 μM ($p = 0.0094$) and 30 μM ($p = 0.0093$) being significantly larger than that seen in VEH-superfused slices. The IC_{50} for (2*R*,6*R*)-HNK to reduce PPR from baseline was 3.8 μM (Fig. 2j).

Next, we sought to test the persistence of the presynaptic potentiation following a period of bath application that roughly approximates the preclinical pharmacokinetic profile of (2*R*,6*R*)-HNK (Fig. 2k) [16]. A 15 min bath application of (2*R*,6*R*)-HNK increased the slope of the fEPSP (Fig. 2m, n; $F_{(4,28)} = 8.129$, $p = 0.0002$, $n = 8$), which was significantly higher than baseline ($p = 0.0039$), and remained elevated in (2*R*,6*R*)-HNK-free ACSF at 45 min ($p < 0.0001$), 75 min ($p = 0.0059$), and 105 min ($p = 0.0929$). In addition, (2*R*,6*R*)-HNK led to a significant reduction in PPR (Fig. 2o; $F_{(4,28)} = 4.283$, $p = 0.0079$), which was significantly lower than at baseline ($p = 0.0265$), and that persisted for at least 45 min in (2*R*,6*R*)-HNK-free ACSF ($p = 0.0048$). Changes in fEPSP slope across the procedure were significantly correlated with changes in PPR (Fig. 2l; $R^2 = 0.4932$, $p < 0.0001$). Overall, these data suggest that (2*R*,6*R*)-HNK enhances AMPAR-mediated synaptic transmission, at least in part, by increasing glutamate release probability.

Enhancing release probability occludes the presynaptic effects of (2*R*,6*R*)-HNK

Removal of extracellular Mg^{2+} augments AMPAR-mediated responses in CA1 through an NMDAR-independent enhancement in glutamate release probability [44]. If (2*R*,6*R*)-HNK increases the probability of glutamate release, then it should also potentiate NMDAR-mediated fEPSPs. However, we previously found that

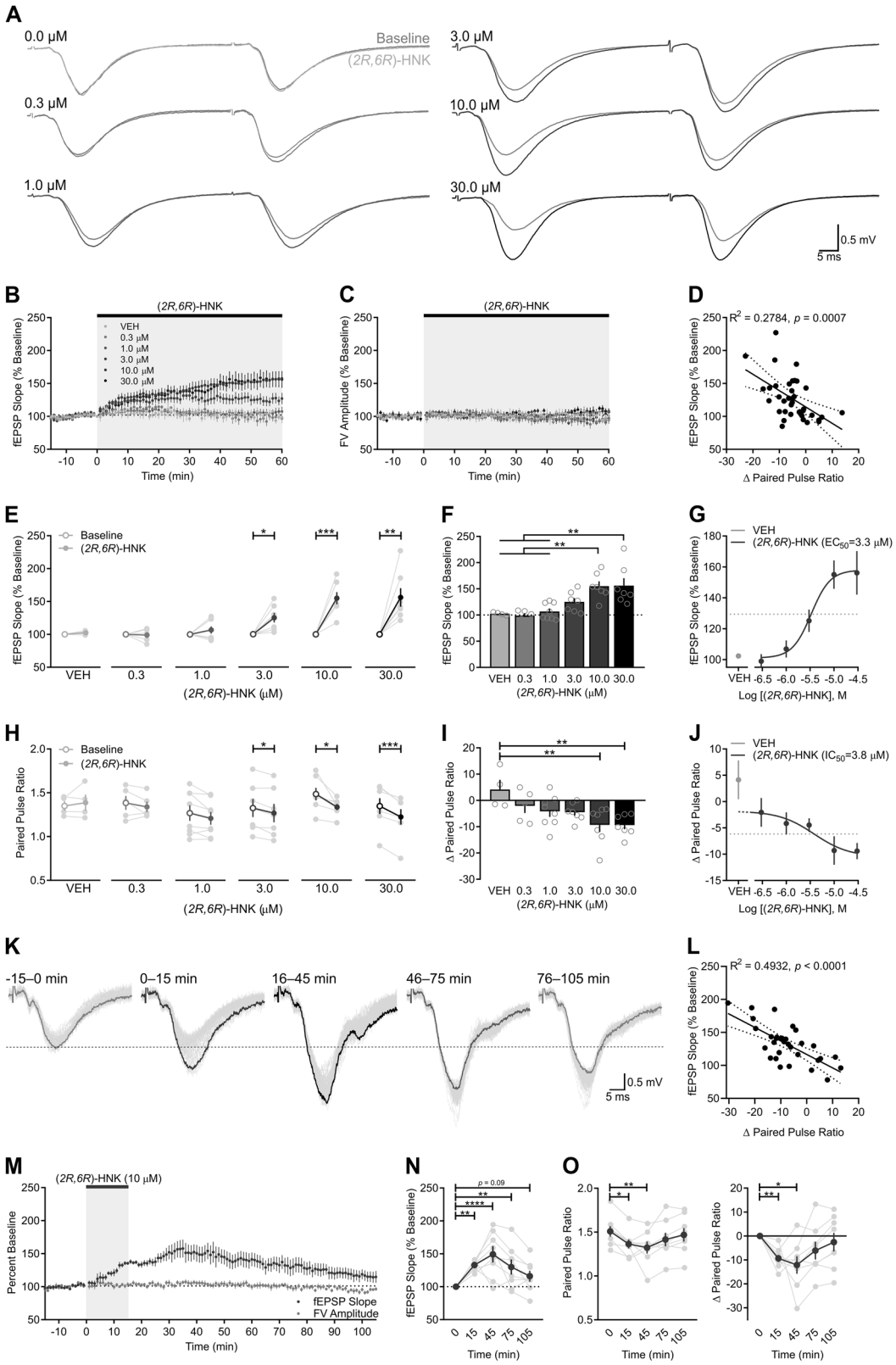
A
0.0 μM
Baseline
(2R,6R)-HNK
0.3 μM
1.0 μM
3.0 μM
10.0 μM
30.0 μM
0.5 mV
5 ms
B
(2R,6R)-HNK
VEH
0.3 μM
1.0 μM
3.0 μM
10.0 μM
30.0 μM
fEPSP Slope (% Baseline)
Time (min)
C
(2R,6R)-HNK
FV Amplitude (% Baseline)
Time (min)
D
R² = 0.2784, p = 0.0007
fEPSP Slope (% Baseline)
Δ Paired Pulse Ratio
E
Baseline
(2R,6R)-HNK
fEPSP Slope (% Baseline)
VEH
0.3
1.0
3.0
10.0
30.0
(2R,6R)-HNK (μM)
F
fEPSP Slope (% Baseline)
VEH 0.3 1.0 3.0 10.0 30.0
(2R,6R)-HNK (μM)
G
VEH
(2R,6R)-HNK (EC50=3.3 μM)
fEPSP Slope (% Baseline)
VEH -6.5 -6.0 -5.5 -5.0 -4.5
Log [(2R,6R)-HNK], M
H
Baseline
(2R,6R)-HNK
Paired Pulse Ratio
VEH
0.3
1.0
3.0
10.0
30.0
(2R,6R)-HNK (μM)
I
Δ Paired Pulse Ratio
VEH 0.3 1.0 3.0 10.0 30.0
(2R,6R)-HNK (μM)
J
VEH
(2R,6R)-HNK (IC50=3.8 μM)
Δ Paired Pulse Ratio
VEH -6.5 -6.0 -5.5 -5.0 -4.5
Log [(2R,6R)-HNK], M
K
-15–0 min
0–15 min
16–45 min
46–75 min
76–105 min
0.5 mV
5 ms
L
R² = 0.4932, p < 0.0001
fEPSP Slope (% Baseline)
Δ Paired Pulse Ratio
M
(2R,6R)-HNK (10 μM)
Percent Baseline
fEPSP Slope
FV Amplitude
Time (min)
N
p = 0.09
fEPSP Slope (% Baseline)
Time (min)
O
Paired Pulse Ratio
Time (min)
Δ Paired Pulse Ratio
Time (min)

Fig. 2 *(2R,6R)-HNK exerts its acute synaptic effects through a concentration-dependent increase in the probability of glutamate release.* **a** Representative paired pulse ratio (PPR) traces generated before ($t = 0$; gray) and after ($t = 60$; blue/black) (*2R,6R*)-hydroxynorketamine (HNK) superfusion. **b** (*2R,6R*)-HNK enhanced field excitatory postsynaptic potentials (fEPSPs) in a concentration-dependent fashion. **c** (*2R,6R*)-HNK did not influence presynaptic fiber volley (FV) amplitude. **d** The fEPSP slope increase induced by (*2R,6R*)-HNK correlated with changes in PPR. Dotted line indicates 95% confidence interval. **e** When compared to baseline (open circles), fEPSP slope increased in the presence of (*2R,6R*)-HNK at 3 μM ($n = 7$), 10 μM ($n = 7$), and 30 μM ($n = 7$) concentrations, but not in the presence of VEH ($n = 4$) or (*2R,6R*)-HNK at 0.3 μM ($n = 5$) or 1 μM ($n = 8$). **f** Ten and 30 μM (*2R,6R*)-HNK increased fEPSP relative to VEH and (*2R,6R*)-HNK at 0.3 or 1 μM conditions. **g** The (*2R,6R*)-HNK-mediated increase in fEPSP $EC_{50} = 3.3$ μM. **h** When compared to baseline, changes in PPR were decreased by (*2R,6R*)-HNK at 3, 10, and 30 μM, but not by VEH or (*2R,6R*)-HNK at 0.3 or 1 μM. **i** Ten and 30 μM (*2R,6R*)-HNK decreased PPR relative to VEH. **j** The (*2R,6R*)-HNK-mediated decrease in PPR $IC_{50} = 3.8$ μM. **k** Representative traces of SC-CA1 fEPSPs. Individual sweeps across the procedure (light gray) are overlaid with terminal averages during baseline (gray), after (*2R,6R*)-HNK superfusion (blue), and during washout with (*2R,6R*)-HNK-free artificial cerebrospinal fluid ($t = 45$, black; $t = 75$, dark gray; $t = 105$, gray). **m** Superfusion of (*2R,6R*)-HNK for 15 min enhanced the slope of SC-CA1 fEPSPs ($n = 8$), **n** which persisted up to 1 h in (*2R,6R*)-HNK-free ACSF, but that was not significantly different from baseline by 1.5 h of washout. The changes in PPR (**o**) were significantly correlated with the magnitude of the fEPSP change induced by (*2R,6R*)-HNK across the procedure (**l**). Dotted line indicates 95% confidence interval. *$p < 0.05$, **$p < 0.01$, ***$p < 0.001$, ****$p < 0.0001$. Points/bars and error bars represent mean and standard error of the mean, respectively

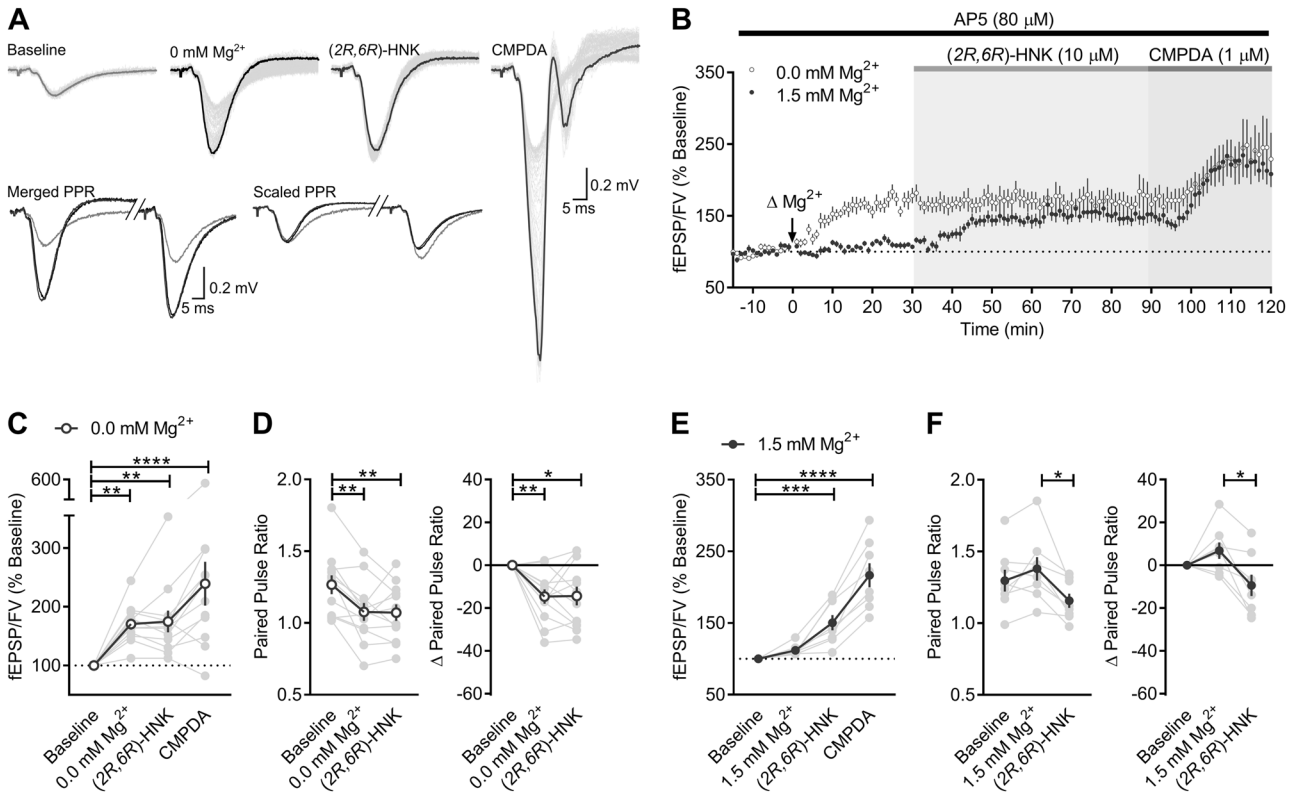

Fig. 3 *Enhancing release probability occludes the presynaptic effects of (2R,6R)-HNK.* **a** Representative traces generated during baseline ($t = 0$; gray), after nominally free magnesium (0 mM Mg^{2+}) artificial cerebrospinal fluid (ACSF) superfusion ($t = 30$; black), (*2R,6R*)-hydroxynorketamine (HNK) superfusion ($t = 90$; blue), and phenyl-1,4-bis-alkylsulfonamide (CMPDA) superfusion (1 μM, $t = 120$; red). Merged and scaled paired pulse ratio (PPR) traces generated during baseline ($t = 0$; gray), after 0 mM Mg^{2+} ACSF superfusion ($t = 30$; black), and after (*2R,6R*)-HNK superfusion ($t = 90$; blue). PPR values were not reported for CMPDA conditions because the late epileptogenic effects of CMPDA prevented accurate measurement of the second fEPSP slope. Recordings were made in the presence of 2-amino-5-phosphonopentanoic acid (AP5, 80 μM). **b** Lowering the concentration of Mg^{2+} acutely potentiated Schaffer collateral (SC)-CA1 field excitatory postsynaptic potentials (fEPSPs, $n = 8$), which occluded further potentiation induced by (*2R,6R*)-HNK under normal Mg^{2+} conditions ($n = 12$), whereas the potentiation induced by the α-amino-3-hydroxy-5-methyl-4-isoxazolepropionic acid receptor (AMPAR) positive allosteric modulator, CMPDA, remained intact. **c** Nominally free Mg^{2+} led to a significant potentiation above baseline, as did the CMPDA-induced potentiation. **d** Nominally free Mg^{2+} significantly reduced PPR from baseline. **e** Under standard Mg^{2+} conditions (1.5 mM), (*2R,6R*)-HNK led to significant potentiation of fEPSPs above baseline, and **f** significantly reduced PPR. *$p < 0.05$, **$p < 0.01$, ***$p < 0.001$, ****$p < 0.0001$. Points/bars and error bars represent mean and standard error of the mean, respectively

(*2R,6R*)-HNK failed to potentiate NMDAR-mediated currents under Mg^{2+}-free conditions [42]. This apparent discrepancy could be reconciled if the (*2R,6R*)-HNK-induced potentiation of NMDAR-mediated responses was occluded by the enhanced release probability produced by removal of Mg^{2+}. We tested this prediction by recording AMPAR-mediated responses from slices superfused with either Mg^{2+}-containing ACSF ($n = 8$) or nominally Mg^{2+}-free ACSF ($n = 12$) prior to their superfusion with (*2R,6R*)-HNK. We tested whether postsynaptically evoked responses are maintained under these conditions by following the (*2R,6R*)-HNK superfusion with application of the AMPAR positive allosteric modulator, phenyl-1,4-bis-alkylsulfonamide [CMPDA, 1 μM; [45]].

As expected, application of Mg^{2+}-free ACSF potentiated AMPAR-mediated fEPSPs and decreased PPR (Fig. 3a, b). There

was a significant main effect of Mg^{2+}-free conditions on the fEPSP slope (Fig. 3c; $F_{(3,33)} = 11.83$, $p < 0.0001$), with removal of Mg^{2+} increasing SC-CA1 fEPSP slopes to 170 ± 9% of baseline ($p = 0.0060$). Under these conditions, (2R,6R)-HNK failed to potentiate responses further (175 ± 9% of baseline), whereas CMPDA significantly enhanced SC-CA1 fEPSPs to 239 ± 37% of baseline ($p = 0.0001$), consistent with its direct postsynaptic actions at AMPARs [45]. There was a significant main effect of nominally free Mg^{2+} on the change in PPR (Fig. 3d; $F_{(2,22)} = 9.658$, $p = 0.0001$), which significantly decreased PPR values from baseline ($p = 0.0017$). Under these conditions, (2R,6R)-HNK failed to decrease PPRs further, suggesting that its presynaptic effects were occluded by the change in release probability that were induced by lowering the concentration of Mg^{2+}. On the other hand, there was a main effect of (2R,6R)-HNK on the change in the fEPSP slope under normal Mg^{2+} conditions (Fig. 3e; $F_{(3,21)} = 39.54$, $p < 0.0001$), with (2R,6R)-HNK potentiating SC-CA1 fEPSPs to 151 ± 11% of baseline ($p = 0.0007$). Similar to nominally free Mg^{2+} conditions, CMPDA potentiated SC-CA1 fEPSPs to 217 ± 16% of baseline ($p < 0.0001$). There was a significant main effect (Fig. 3f; $F_{(2,14)} = 7.277$, $p = 0.0068$) for the change in PPR induced by (2R,6R)-HNK ($p = 0.0062$). Thus, we conclude that the nominal absence of Mg^{2+} occluded the presynaptic plasticity induced by (2R,6R)-HNK, and likely accounts for the failure to observe the (2R,6R)-HNK-induced potentiation of NMDAR-mediated fEPSPs reported previously [42]. The finding that (2R,6R)-HNK-induced potentiation was occluded by disinhibiting glutamate release probability supports that (2R,6R)-HNK is acting presynaptically to exert its effects on AMPAR-mediated synaptic transmission. However, given that PPR can be additionally influenced by postsynaptic events, and also does not independently rule out whether an additional postsynaptic mechanism is involved, we next examined the effects of (2R,6R)-HNK on miniature synaptic transmission.

(2R,6R)-HNK increases the frequency, but not amplitude, of mEPSCs

There are shared mechanisms mediating evoked and spontaneous release of glutamate [46, 47]. If (2R,6R)-HNK acts at the presynaptic terminal to enhance glutamatergic release probability, then it should also produce an increase in the frequency of mEPSCs recorded in the presence of TTX (0.3 μM; Fig. 4a). If (2R,6R)-HNK acts postsynaptically to enhance glutamatergic transmission, then it should increase mEPSC amplitude. Consistent with a presynaptic mechanism of action, there were significant main effects of (2R,6R)-HNK ($F_{(1,14)} = 6.345$, $p = 0.0246$) and time ($F_{(6,84)} = 4.197$, $p = 0.0010$), as well as a significant interaction between the two factors ($F_{(6,\ 84)} = 3.069$, $p = 0.0092$) on mEPSC frequency (Fig. 4b). When compared to baseline, (2R,6R)-HNK significantly increased the frequency of mEPSCs by the 15–20 min ($p = 0.0042$) and 20–25 min ($p = 0.0007$) time-bins (Fig. 4b), wherein mEPSC frequency was significantly higher in the presence of (2R,6R)-HNK than in the presence of VEH ($p = 0.0081$ and $p = 0.0020$, respectively). Consistent with this, (2R,6R)-HNK perfusion was associated with a significant leftward shift in the cumulative distribution of interevent intervals when compared to baseline (Fig. 4d; Kolmogorov–Smirnov [KS] = 0.1560, $p = 0.0046$), whereas no differences were observed in VEH-treated conditions (Fig. 4c; KS = 0.0880, $p = 0.2877$). The mEPSCs recorded here were solely mediated by AMPARs as they were abolished by superfusion of slices with ACSF containing the AMPAR antagonist, 6-cyano-7-nitroquinoxaline-2,3-dione (CNQX, 10 μM; Fig. 4a). While by 15–20 min superfusion, (2R,6R)-HNK significantly increased mEPSC frequency when compared to VEH control (Fig. 4b; $t_{(17)} = 2.385$, $p = 0.0290$, *right panel*) and baseline (Fig. 4d; $t_{(8)} = 4.094$, $p = 0.0035$, *right panel*), it had no significant effect on mEPSC amplitude when compared to VEH (Fig. 4e; $t_{(17)} = 0.7892$, $p = 0.4409$, *right panel*) or baseline (Fig. 4g; $t_{(5)} = 1.149$, $p = 0.3026$, *right panel*). Consistent with this, no differences were observed from baseline in the cumulative distribution of mEPSC amplitudes in VEH- (Fig. 4f; KS = 0.0600, $p = 0.7591$) or (2R,6R)-HNK-exposed slices (Fig. 4g; KS = 0.0920, $p = 0.2406$). These results support the conclusion that (2R,6R)-HNK potentiates excitatory synaptic transmission by increasing glutamate release probability.

The presynaptic effects of (2R,6R)-HNK occur at Schaffer collateral synapses, but not at temporoammonic synapses

The processes that regulate vesicular release are diverse among excitatory synapses [48, 49], even within the CA1 field of the hippocampus [50, 51]. Thus, if the synaptic effects of (2R,6R)-HNK are mediated by a selective enhancement in glutamate release, then its effects may vary as a function of the presynaptic afferent being stimulated. To test this prediction, a dual stimulation protocol was used to apply alternating stimulation to SC and temporoammonic (TA) afferents, respectively, which converge onto the same population of CA1 neurons (Fig. 5a). TA-CA1 synapses are formed in the stratum lacunosum-moleculare region of CA1, and project from layer III of the entorhinal cortex. In the SC-CA1 pathway (Fig. 5b), (2R,6R)-HNK potentiated fEPSPs to 165 ± 9% of baseline (Fig. 5c, d; $t_{(9)} = 7.046$, $p = 0.0001$, $n = 10$) and significantly reduced PPR (Fig. 5e; $t_{(9)} = 5.39$, $p = 0.0004$), whereas no change in either fEPSP ($t_{(4)} = 0.3932$, $p = 0.7142$, $n = 5$) or PPR ($t_{(4)} = 1.409$, $p = 0.2317$, *data not shown*) were observed in the VEH-treated condition. By contrast, in the TA-CA1 pathway (Fig. 5f), (2R,6R)-HNK failed to potentiate fEPSPs (Fig. 5g, h; $t_{(9)} = 0.9968$, $p = 0.3573$) or suppress PPR (Fig. 5i; $t_{(9)} = 0.3894$, $p = 0.7061$); no change in either fEPSP ($t_{(4)} = 1.552$, $p = 0.1956$) or PPR ($t_{(4)} = 0.5895$, $p = 0.5872$) were observed in the VEH-treated condition (*data not shown*). There were significant main effects of treatment ($F_{(1,13)} = 16.05$, $p = 0.0015$) and synapse ($F_{(1,13)} = 23.17$, $p = 0.0003$) on the fEPSP slope, and a treatment × synapse interaction ($F_{(1,13)} = 25.94$, $p = 0.0002$; Fig. 5j). Specifically, there was a significant fEPSP increase in (2R,6R)-HNK-exposed SC-CA1 synapses relative to VEH-exposed SC-CA1 synapses ($p < 0.0001$) and (2R,6R)-HNK-exposed TA-CA1 synapses ($p < 0.0001$). The treatment × synapse interaction for the effect of (2R,6R)-HNK on the change in PPR did not reach statistical significance (Fig. 5k; $F_{(1,13)} = 1.224$, $p = 0.2887$); however, planned comparisons revealed significant differences between VEH and (2R,6R)-HNK-treated slices in the SC-CA1 pathway ($p = 0.0384$), and between the SC-CA1 and TA-CA1 pathways for (2R,6R)-HNK-treated slices ($p = 0.0296$).

DISCUSSION

Rapid-acting antidepressants are proposed to exert their effects by restoring the balance of synaptic excitation to inhibition throughout mesocorticolimbic circuits [18, 26–28]. Preclinical studies have shown that, similar to ketamine [24, 29, 52], (2R,6R)-HNK causes enduring alterations in synaptic function throughout the brain and in behavioral tests that are used to predict antidepressant efficacy [30–34, 36, 38, 39]. Despite this, the mechanisms underlying the synaptic effects of (2R,6R)-HNK remain largely unknown. The results presented here demonstrate for the first time that (2R,6R)-HNK acts presynaptically at SC terminals to acutely enhance glutamatergic transmission in the CA1 field of the hippocampus. In addition, this potentiation is distinct from canonical forms of NMDAR-dependent long-term potentiation at SC synapses [53], as the acute plasticity induced by (2R,6R)-HNK was expressed presynaptically and occurred in the presence of NMDAR blockade.

A previous study from our laboratory suggests that (2R,6R)-HNK contributes to the antidepressant-like effects of ketamine [30], with ketamine's in vivo effects being more potently expressed in female rodents when compared to males [30, 54]. However, here

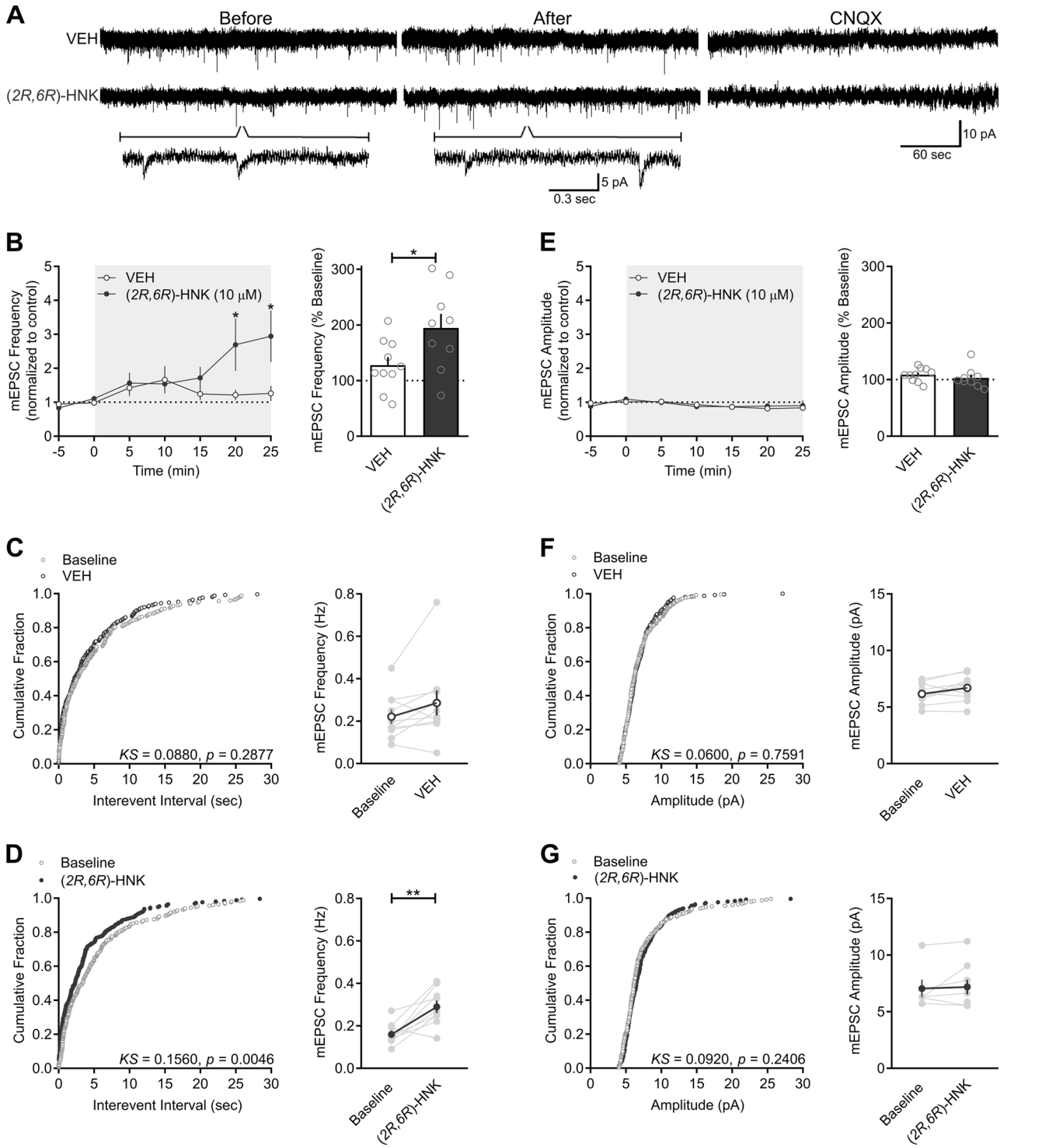

Fig. 4 *(2R,6R)-HNK increases the frequency, but not amplitude, of mEPSCs*. **a** Representative sample recordings of miniature excitatory postsynaptic currents (mEPSCs) recorded for 5 min before and 20 min after the beginning of superfusion of hippocampal slices with vehicle (VEH)- or (*2R,6R*)-hydroxynorketamine (HNK)-containing artificial cerebrospinal fluid (ACSF) that contained tetrodotoxin (TTX, 0.3 μM). Traces in the compressed time scale provide a representation of the frequency of events before and after (*2R,6R*)-HNK bath application, whereas the traces in the expanded scale provide a representation of the overall kinetics of events. **b** Frequency of monosynaptically generated mEPSCs recorded in the presence of (*2R,6R*)-HNK (10 μM) increased significantly with time, and the effect became significant at 15–20 min after the beginning of the superfusion ($n = 6$, *left panel*). Frequency of mEPSCs recorded at 15–20 min after beginning of superfusion of 10 slices with (*2R,6R*)-HNK-containing ACSF was significantly larger than that recorded from VEH-superfused slices (*right panel*). **c** Cumulative distribution of interevent intervals were unchanged from baseline in VEH conditions, whereas **d** there was a significant leftward shift after (*2R,6R*)-HNK exposure relative to baseline. **e** mEPSC amplitude was unaltered in either **f** VEH or **g** (*2R,6R*)-HNK-exposed slices. Only cells from which mEPSCs were continuously recorded for 25 min were included in panels **b** and **e**. $^{*}p < 0.05$, $^{**}p < 0.01$. Points/bars and error bars represent mean and standard error of the mean, respectively

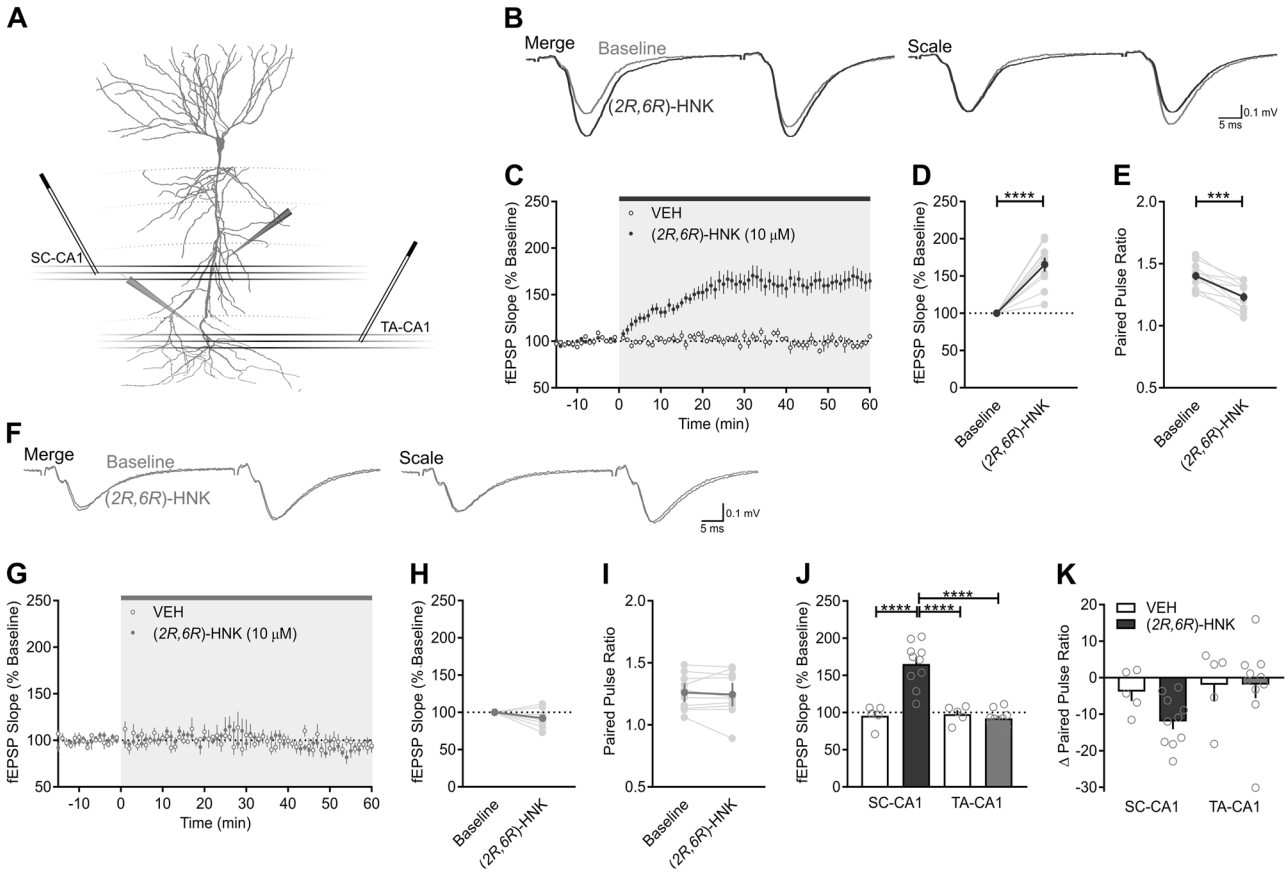

Fig. 5 *The presynaptic effects of (2R,6R)-HNK occur at Schaffer collateral synapses, but not at temporoammonic synapses.* **a** Schematic of the dual extracellular recording arrangement [pyramidal cell outline adapted from [57]]. Both SC and TA afferents were stimulated in an alternating fashion, and recording pipettes were placed in stratum radiatum and stratum lacunosum-moleculare of CA1, respectively. **b** Representative paired pulse ratio (PPR) traces generated before ($t = 0$; gray) and after ($t = 60$; blue) (*2R,6R*)-hydroxynorketamine (HNK) superfusion in SC-CA1. **c** (*2R,6R*)-HNK (10 μM, $n = 10$) enhanced SC-CA1 field excitatory postsynaptic potentials (fEPSPs) when compared to vehicle (VEH)-treated control slices ($n = 5$). **d** The (*2R,6R*)-HNK-induced potentiation of SC-CA1 fEPSPs was significant when compared to baseline, whereas no changes in VEH-exposed slices were observed (*data not shown*). **e** (*2R,6R*)-HNK significantly reduced PPR in SC-CA1; no changes in VEH-exposed slices were observed (*data not shown*). **f** Representative PPR traces generated before ($t = 0$; gray) and after ($t = 60$; green) (*2R,6R*)-HNK superfusion in the TA-CA1 pathway. **g** (*2R,6R*)-HNK had no effect on TA-CA1 fEPSPs. **h** The effect of (*2R,6R*)-HNK on fEPSP slope at TA-CA1 synapses was not significantly different from baseline. **i** (*2R,6R*)-HNK did not influence PPR at TA-CA1 synapses. **j** The (*2R,6R*)-HNK-induced potentiation of SC-CA1 fEPSPs was significantly higher than at VEH-exposed SC-CA1 synapses and (*2R,6R*)-HNK-exposed TA-CA1 synapses. **k** The (*2R,6R*)-HNK-induced decrease in PPR at SC-CA1 synapses was lower than at VEH-exposed SC-CA1 synapses and (*2R,6R*)-HNK-exposed TA-CA1 synapses. ***$p < 0.001$, ****$p < 0.0001$. Points/bars and error bars represent mean and standard error of the mean, respectively

we report that (*2R,6R*)-HNK similarly enhanced glutamatergic transmission in male and female hippocampal slices at 10 μM—a concentration approximating peak extracellular hippocampal levels following antidepressant dosing of (*2R,6R*)-HNK (10 mg/kg) in male mice [42]. Consequently, the current finding that potentiation of SC-CA1 synaptic transmission by (*2R,6R*)-HNK is sex-independent suggests that the direct actions of (*2R,6R*)-HNK on excitatory transmission do not explain these sex-dependent behavioral effects of ketamine. In addition, we conclude that organizational sex differences are not present, considering the prepubertal age of the female rats used, although, we cannot fully exclude that activational effects of female gonadal hormones could play a role. Conducting a similar study in older, cycling females would be needed to address whether the estrous cycle modulates the potentiation induced by (*2R,6R*)-HNK.

The potentiation induced by (*2R,6R*)-HNK at SC-CA1 synapses was concentration-dependent (3–30 μM), with a concentration of 10 μM (*2R,6R*)-HNK yielding a similar magnitude of potentiation in dorsal (155%; Fig. 2) and ventral (165%; Fig. 5) hippocampus. Notably, these effective concentrations of (*2R,6R*)-HNK are relevant to its antidepressant-like actions in preclinical studies. For example, mice treated with 10 mg/kg of (*2R,6R*)-HNK display ketamine-like antidepressant responses in the forced swim, learned helplessness, and novelty suppressed feeding tests, as well as sucrose and female urine preference tests following chronic corticosterone administration [30, 38, 39, 42]. At a 10 mg/kg dose, extracellular hippocampal concentrations peak at ~8 μM [42], which are compatible with concentrations of (*2R,6R*)-HNK that potentiate fEPSPs in the current study (EC_{50} of 3.3 μM; Fig. 2g). We also note that this EC_{50} is consistent with the maximal estimated unbound brain (*2R,6R*)-HNK concentrations (0.92–4.84 μM) calculated from effective doses of ketamine in rodents, but above its projected maximal human levels (≤37.8 ± 14.3 nM) following administration of ketamine at antidepressant doses [55]. In addition, potentiation of glutamatergic transmission by (*2R,6R*)-HNK was observed in the presence of the NMDAR inhibitor, AP5, and therefore did not require NMDAR activity. This is consistent with earlier studies reporting that (*2R,6R*)-HNK only blocks NMDARs at concentrations higher than those reported here to potentiate AMPAR-mediated fEPSPs [30, 40, 43]. In fact, under experimental conditions similar to the current study, (*2R,6R*)-HNK inhibited NMDAR-mediated fEPSPs at SC-CA1 synapses with an IC_{50} of 212 μM [42].

The potentiation of AMPAR-mediated fEPSPs by (2R,6R)-HNK was accompanied by a decrease in PPR, suggesting that (2R,6R)-HNK increases glutamate release probability. We tested the persistence of the potentiation following a period of bath application that roughly approximates the pharmacokinetic profile of (2R,6R)-HNK following an effective 10 mg/kg dose administered to mice [30, 42]. Specifically, we have recently shown that maximum extracellular hippocampal concentrations reach ~8 μM at 10 and 20 min following intraperitoneal administration of an antidepressant-relevant dose of 10 mg/kg [42]. The rate of clearance of (2R,6R)-HNK from the hippocampus is rapid, with ~3 μM remaining by 30 min post injection and ~0.3 μM by 60 min. Here, we report that 15 min bath application of (2R,6R)-HNK led to a potentiation that remained an hour in (2R,6R)-HNK-free ACSF. We note that at 90 min following washout there was no significant difference from baseline ($p = 0.09$). Given that the pharmacokinetic profile of (2R,6R)-HNK shows that it has a rapid half-life and no brain-selective accumulation following systemic administration in vivo [42], it is likely that (2R,6R)-HNK is rapidly cleared when slices are superfused with (2R,6R)-HNK-free ACSF. However, it is also possible that high-affinity target binding contributes to the persistent effect we observe.

We also found that (2R,6R)-HNK enhanced the frequency, but not amplitude, of mEPSCs recorded from CA1 pyramidal neurons, further supporting a presynaptic site of action. One hypothesis for how ketamine is proposed to exert its antidepressant effects is to disinhibit excitatory synaptic transmission by selectively inhibiting NMDARs localized on GABAergic inhibitory interneurons [19–21]. However, our effects of (2R,6R)-HNK on mEPSCs were observed in the presence of the sodium channel blocker, TTX, which prevents action potential generation, indicating that GABAergic disinhibition of glutamatergic transmission is not required for the (2R,6R)-HNK-induced increases in AMPAR-mediated mEPSC frequency. In addition, similar to a recent conclusion by Shaffer et al. [55], our data indicate that (2R,6R)-HNK does not directly activate AMPARs, given that the amplitude of miniature events was unchanged. Interestingly, an extracellular dual stimulation protocol revealed that the (2R,6R)-HNK-induced presynaptic potentiation of fEPSPs was synapse-specific, as it was observed at SC-CA1, but not TA-CA1 synapses. While our whole-cell experiments do not definitely test through which synaptic input (2R,6R)-HNK is exerting its effects on mEPSC frequency, it is likely that the mEPSCs recorded from the soma of CA1 pyramidal neurons are mediated primarily by glutamate released from SC rather than TA terminals. This is because TA-CA1 synapses are electrotonically remote from the soma of those neurons, and are largely outnumbered by SC-CA1 synapses [56–59]. While the exact mechanism by which (2R,6R)-HNK exerts its synapse-specific effects remains to be determined, our results suggest that (2R,6R)-HNK selectively targets a presynaptic mechanism that specifically regulates glutamate release in SC-CA1 synapses but not in TA-CA1 synapses under these recording conditions. Importantly, there are topographically distinct TA-CA1 projections with marked differences in presynaptic protein expression and function [56], and TA synapses have been shown to express a form of long-term potentiation that involves the recruitment of presynaptic N-type calcium channels [51]. It is possible that differences in the molecular mechanisms that regulate vesicular release between these SC-CA1 and TA-CA1 synapses endow (2R,6R)-HNK with a selective effect on SC-CA1 synapses, for instance, through differential expression of presynaptic calcium channel subtypes [51].

Enduring alterations in AMPAR-dependent synaptic transmission are thought to underlie the antidepressant-relevant behavioral effects of (2R,6R)-HNK [30–38]. It is important to note that the mechanisms underlying the acute presynaptic effects of (2R,6R)-HNK in hippocampal slices may be distinct from the sustained adaptations in synaptic efficacy that yield persistent antidepressant-like behavioral responses in vivo. For instance, while both the rapid and sustained antidepressant-like behavioral effects of (2R,6R)-HNK require AMPAR activation, hippocampal synaptic AMPAR protein levels are upregulated 24 h, but not 1 h, after systemic administration [30]. This is consistent with the delayed expression of AMPAR-dependent structural plasticity following submicromolar (2R,6R)-HNK exposure in vitro [35], and resembles enduring forms of synaptic plasticity that rely on de novo protein synthesis [60]. Given the apparent reversal of (2R,6R)-HNK's acute presynaptic effects in the current study, our data suggest that an acute presynaptically-mediated change in fast excitation could induce a secondary, delayed postsynaptic increase in AMPAR expression, thereby accounting for the persistent behavioral actions of (2R,6R)-HNK.

There is mounting evidence that the in vivo effects of (2R,6R)-HNK could be mediated by diverse actions throughout the brain. For instance, while (2R,6R)-HNK's acute effects appear to be mediated presynaptically in the hippocampus, bath application of (2R,6R)-HNK (10 μM), and systemic (2R,6R)-HNK administration (10 mg/kg, i.p.), induces rapid pre- and postsynaptic adaptations within the ventrolateral periaqueductal gray (vlPAG), which are also AMPAR-dependent [34]. Like the hippocampus, the vlPAG is subject to stress-induced impairments in glutamatergic transmission that are thought to contribute to the emergence of depressive-like behaviors in rodents [61], and that are responsive to the effects of (2R,6R)-HNK in vivo and ex vivo [34]. Similarly, within-medial prefrontal cortex (2R,6R)-HNK infusion produces brain-derived neurotrophic factor-tropomyosin receptor kinase B-dependent antidepressant-relevant actions comparable to systemically administered (2R,6R)-HNK [38], possibly through a sustained enhancement in extracellular glutamate levels [31]. In contrast, both ketamine and (2R,6R)-HNK reduce synaptic potentiation and AMPAR function in the ventral tegmental area-nucleus accumbens circuit [32]. Additional circuit-level investigations conducted in vivo will help to unify the diverse actions of (2R,6R)-HNK throughout the mesocorticolimbic system.

There remains some debate regarding the role of ketamine metabolites in the therapeutic antidepressant actions of ketamine [62]. Nevertheless, (2R,6R)-HNK has been shown to exert actions similar to ketamine in preclinical models of antidepressant efficacy and depressive-like behavior [30, 31, 34, 38, 39]. In addition, (2R,6R)-HNK displays less evidence of adverse effects in comparison to ketamine in preclinical studies [30, 39]. The current results provide critical insights regarding (2R,6R)-HNK's mechanism of action, implicating immediate, synapse-selective, presynaptically mediated changes in synaptic strength. These findings advance a mechanistic framework for the development of improved therapeutic options for depression.

FUNDING AND DISCLOSURE

This research was supported by NIH/NIGMS T32-GM008181 (to LMR), NIH/NINDS T32-NS063391 (to LMR), NIH/NIGMS R25-GM055036 (to LMR), NIH/NIMH R01-MH086828 (to SMT), NIH/NIMH R01-MH107615 (to TDG), a Harrington Project for Discovery and Development Scholar Innovator Award (to TDG), and a U.S. Department of Veterans Affairs Merit Award 1I01BX004062 (to TDG). The contents of this manuscript do not represent the views of the U.S. Department of Veterans Affairs or the United States Government. TDG has received research funding from Allergan, Janssen, and Roche Pharmaceuticals during the preceding 3 years and is a consultant for FSV7 LLC. PZ and TDG are listed as co-inventors on a patent application for the use of (2R,6R)-hydroxynorketamine in the treatment of depression, anxiety, anhedonia, suicidal ideation, and post-traumatic stress disorders. PZ and TDG have assigned their patent rights to the University of Maryland, Baltimore, but will share a percentage of any royalties that may be received by the University of Maryland, Baltimore. LMR, YA, JF, EXA, EFRP, and SMT declare no competing interests.

ACKNOWLEDGEMENTS

LMR performed the extracellular electrophysiology experiments and analyzed data; YA performed the whole-cell electrophysiology experiments analyzed by YA, PZ, and EFRP; JF conducted preliminary experiments; LMR, PZ, EXA, EFRP, SMT, and TDG designed the research; LMR and TDG wrote the manuscript. We thank Craig J. Thomas and Patrick J. Morris (National Center for Advancing Translational Sciences) for providing the (*2R,6R*)-HNK.

ADDITIONAL INFORMATION

Supplementary Information accompanies this paper at (https://doi.org/10.1038/s41386-019-0443-3).

Publisher's note: Springer Nature remains neutral with regard to jurisdictional claims in published maps and institutional affiliations.

REFERENCES

1. Vos T, Abajobir AA, Abbafati C, Abbas KM, Abate KH, Abd-Allah F, et al. Global, regional, and national incidence, prevalence, and years lived with disability for 328 diseases and injuries for 195 countries, 1990-2016: a systematic analysis for the Global Burden of Disease Study 2016. Lancet. 2017;390:1211–59.
2. Jakobsen JC, Katakam KK, Schou A, Hellmuth SG, Stallknecht SE, Leth-Moller K, et al. Selective serotonin reuptake inhibitors versus placebo in patients with major depressive disorder. a systematic review with meta-analysis and trial sequential analysis. BMC Psychiatry. 2017;17:58.
3. Berman RM, Cappiello A, Anand A, Oren DA, Heninger GR, Charney DS, et al. Antidepressant effects of ketamine in depressed patients. Biol Psychiatry. 2000;47:351–4.
4. Zarate CA Jr., Singh JB, Carlson PJ, Brutsche NE, Ameli R, Luckenbaugh DA, et al. A randomized trial of an N-methyl-D-aspartate antagonist in treatment-resistant major depression. Arch Gen Psychiatry. 2006;63:856–64.
5. Feder A, Parides MK, Murrough JW, Perez AM, Morgan JE, Saxena S, et al. Efficacy of intravenous ketamine for treatment of chronic posttraumatic stress disorder: a randomized clinical trial. JAMA Psychiatry. 2014;71:681–8.
6. DiazGranados N, Ibrahim LA, Brutsche NE, Ameli R, Henter ID, Luckenbaugh DA, et al. Rapid resolution of suicidal ideation after a single infusion of an N-methyl-D-aspartate antagonist in patients with treatment-resistant major depressive disorder. J Clin Psychiatry. 2010;71:1605–11.
7. Price RB, Iosifescu DV, Murrough JW, Chang LC, Al Jurdi RK, Iqbal SZ, et al. Effects of ketamine on explicit and implicit suicidal cognition: a randomized controlled trial in treatment-resistant depression. Depress Anxiety. 2014;31:335–43.
8. Murrough JW, Soleimani L, DeWilde KE, Collins KA, Lapidus KA, Iacoviello BM, et al. Ketamine for rapid reduction of suicidal ideation: a randomized controlled trial. Psychol Med. 2015;45:3571–80.
9. Bloch MH, Wasylink S, Landeros-Weisenberger A, Panza KE, Billingslea E, Leckman JF, et al. Effects of ketamine in treatment-refractory obsessive-compulsive disorder. Biol Psychiatry. 2012;72:964–70.
10. Rodriguez CI, Kegeles LS, Levinson A, Feng T, Marcus SM, Vermes D, et al. Randomized controlled crossover trial of ketamine in obsessive-compulsive disorder: proof-of-concept. Neuropsychopharmacology. 2013;38:2475–83.
11. Lally N, Nugent AC, Luckenbaugh DA, Niciu MJ, Roiser JP, Zarate CA Jr. Neural correlates of change in major depressive disorder anhedonia following open-label ketamine. J Psychopharmacol. 2015;29:596–607.
12. Ballard ED, Wills K, Lally N, Richards EM, Luckenbaugh DA, Walls T, et al. Anhedonia as a clinical correlate of suicidal thoughts in clinical ketamine trials. J Affect Disord. 2017;218:195–200.
13. Krystal JH, Karper LP, Seibyl JP, Freeman GK, Delaney R, Bremner JD, et al. Subanesthetic effects of the noncompetitive NMDA antagonist, ketamine, in humans. Psychotomimetic, perceptual, cognitive, and neuroendocrine responses. Arch Gen Psychiatry. 1994;51:199–214.
14. Short B, Fong J, Galvez V, Shelker W, Loo CK. Side-effects associated with ketamine use in depression: a systematic review. Lancet Psychiatry. 2017;5:65–78.
15. Sassano-Higgins S, Baron D, Juarez G, Esmaili N, Gold M. A review of ketamine abuse and diversion. Depress Anxiety. 2016;33:718–27.
16. Zanos P, Moaddel R, Morris PJ, Riggs LM, Highland JN, Georgiou P, et al. Ketamine and ketamine metabolite pharmacology: insights into therapeutic mechanisms. Pharm Rev. 2018;70:621–60.
17. Kadriu B, Musazzi L, Henter ID, Graves M, Popoli M, Zarate CA Jr. Glutamatergic neurotransmission: pathway to developing novel rapid-acting antidepressant treatments. Int J Neuropsychopharmacol. 2018;22:119–35.
18. Zanos P, Thompson SM, Duman RS, Zarate CA Jr., Gould TD. Convergent mechanisms underlying rapid antidepressant action. CNS Drugs. 2018;32:197–227.
19. Moghaddam B, Adams B, Verma A, Daly D. Activation of glutamatergic neurotransmission by ketamine: a novel step in the pathway from NMDA receptor blockade to dopaminergic and cognitive disruptions associated with the prefrontal cortex. J Neurosci. 1997;17:2921–7.
20. Widman AJ, McMahon LL. Disinhibition of CA1 pyramidal cells by low-dose ketamine and other antagonists with rapid antidepressant efficacy. Proc Natl Acad Sci USA. 2018;115:E3007–16.
21. Duman RS. Ketamine and rapid-acting antidepressants: a new era in the battle against depression and suicide. F1000Research. 2018;7:pii: F1000.
22. Miller OH, Yang L, Wang CC, Hargroder EA, Zhang Y, Delpire E, et al. GluN2B-containing NMDA receptors regulate depression-like behavior and are critical for the rapid antidepressant actions of ketamine. eLife. 2014;3:e03581.
23. Nosyreva E, Szabla K, Autry AE, Ryazanov AG, Monteggia LM, Kavalali ET. Acute suppression of spontaneous neurotransmission drives synaptic potentiation. J Neurosci. 2013;33:6990–7002.
24. Autry AE, Adachi M, Nosyreva E, Na ES, Los MF, Cheng PF, et al. NMDA receptor blockade at rest triggers rapid behavioural antidepressant responses. Nature. 2011;475:91–5.
25. Newport DJ, Carpenter LL, McDonald WM, Potash JB, Tohen M, Nemeroff CB. Ketamine and other NMDA antagonists: early clinical trials and possible mechanisms in depression. Am J Psychiatry. 2015;172:950–66.
26. Thompson SM, Kallarackal AJ, Kvarta MD, Van Dyke AM, LeGates TA, Cai X. An excitatory synapse hypothesis of depression. Trends Neurosci. 2015;38:279–94.
27. Murrough JW, Abdallah CG, Mathew SJ. Targeting glutamate signalling in depression: progress and prospects. Nat Rev Drug Disco. 2017;16:472–86.
28. Abdallah CG, Sanacora G, Duman RS, Krystal JH. The neurobiology of depression, ketamine and rapid-acting antidepressants: is it glutamate inhibition or activation? Pharm Ther. 2018;190:148–58.
29. Maeng S, Zarate CA Jr., Du J, Schloesser RJ, McCammon J, Chen G, et al. Cellular mechanisms underlying the antidepressant effects of ketamine: role of alpha-amino-3-hydroxy-5-methylisoxazole-4-propionic acid receptors. Biol Psychiatry. 2008;63:349–52.
30. Zanos P, Moaddel R, Morris PJ, Georgiou P, Fischell J, Elmer GI, et al. NMDAR inhibition-independent antidepressant actions of ketamine metabolites. Nature. 2016;533:481–6.
31. Pham TH, Defaix C, Xu X, Deng SX, Fabresse N, Alvarez JC, et al. Common neurotransmission recruited in (*R,S*)-ketamine and (*2R,6R*)-hydroxynorketamine-induced sustained antidepressant-like effects. Biol Psychiatry. 2018;84:e3–6.
32. Yao N, Skiteva O, Zhang X, Svenningsson P, Chergui K. Ketamine and its metabolite (*2R,6R*)-hydroxynorketamine induce lasting alterations in glutamatergic synaptic plasticity in the mesolimbic circuit. Mol Psychiatry. 2018;23:2066–77.
33. Cavalleri L, Merlo Pich E, Millan MJ, Chiamulera C, Kunath T, Spano PF, et al. Ketamine enhances structural plasticity in mouse mesencephalic and human iPSC-derived dopaminergic neurons via AMPAR-driven BDNF and mTOR signaling. Mol Psychiatry. 2018;23:812–23.
34. Chou D, Peng HY, Lin TB, Lai CY, Hsieh MC, Wen YC, et al. *2R,6R*)-hydroxynorketamine rescues chronic stress-induced depression-like behavior through its actions in the midbrain periaqueductal gray. Neuropharmacology. 2018;139:1–12.
35. Collo G, Cavalleri L, Chiamulera C, Merlo Pich E. *2R,6R*)-hydroxynorketamine promotes dendrite outgrowth in human inducible pluripotent stem cell-derived neurons through AMPA receptor with timing and exposure compatible with ketamine infusion pharmacokinetics in humans. Neuroreport. 2018;29:1425–30.
36. Ho MF, Correia C, Ingle JN, Kaddurah-Daouk R, Wang L, Kaufmann SH, et al. Ketamine and ketamine metabolites as novel estrogen receptor ligands: induction of cytochrome P450 and AMPA glutamate receptor gene expression. Biochem Pharm. 2018;152:279–92.
37. Wray NH, Schappi JM, Singh H, Senese NB, Rasenick MM. NMDAR-independent, cAMP-dependent antidepressant actions of ketamine. Mol Psychiatry. 2018; https://doi.org/10.1038/s41380-018-0083-8. [published ahead of print].
38. Fukumoto K, Fogaca MV, Liu R, Duman CH, Kato T, Li X, et al. Activity-dependent brain-derived neurotrophic factor signaling is required for the antidepressant actions of (*2R,6R*)-hydroxynorketamine. Proc Natl Acad Sci USA. 2019;116:297–302.
39. Highland JN, Morris PJ, Zanos P, Lovett J, Ghosh S, Wang AQ, et al. Mouse, rat, and dog bioavailability and mouse oral antidepressant efficacy of (2R,6R)-hydroxynorketamine. J Psychopharmacol. 2018;29:269881118812095.
40. Suzuki K, Nosyreva E, Hunt KW, Kavalali ET, Monteggia LM. Effects of a ketamine metabolite on synaptic NMDAR function. Nature. 2017;546:E1–3.
41. Zanos P, Moaddel R, Morris PJ, Georgiou P, Fischell J, Elmer GI, et al. Zanos et al. reply. Nature. 2017;546:E4–5.
42. Lumsden EW, Troppoli TA, Myers SJ, Zanos P, Aracava Y, Kehr J. et al. Antidepressant-relevant concentrations of the ketamine metabolite (*2R,6R*)-hydroxynorketamine do not block NMDA receptor function. Proc Natl Acad Sci USA. 2019;116:5160–69.

43. Morris PJ, Moaddel R, Zanos P, Moore CE, Gould T, Zarate CA Jr., et al. Synthesis and N-methyl-D-aspartate (NMDA) receptor activity of ketamine metabolites. Org Lett. 2017;19:4572–5.
44. Hamon B, Stanton PK, Heinemann U. An N-methyl-D-aspartate receptor-independent excitatory action of partial reduction of extracellular [Mg2+] in CA1-region of rat hippocampal slices. Neurosci Lett. 1987;75:240–5.
45. Timm DE, Benveniste M, Weeks AM, Nisenbaum ES, Partin KM. Structural and functional analysis of two new positive allosteric modulators of GluA2 desensitization and deactivation. Mol Pharm. 2011;80:267–80.
46. Ramirez DM, Kavalali ET. Differential regulation of spontaneous and evoked neurotransmitter release at central synapses. Curr Opin Neurobiol. 2011;21:275–82.
47. Kaeser PS, Regehr WG. Molecular mechanisms for synchronous, asynchronous, and spontaneous neurotransmitter release. Annu Rev Physiol. 2014;76:333–63.
48. O'Rourke NA, Weiler NC, Micheva KD, Smith SJ. Deep molecular diversity of mammalian synapses: why it matters and how to measure it. Nat Rev Neurosci. 2012;13:365–79.
49. Chamberland S, Toth K. Functionally heterogeneous synaptic vesicle pools support diverse synaptic signalling. J Physiol. 2016;594:825–35.
50. Qian J, Noebels JL. Presynaptic Ca2+channels and neurotransmitter release at the terminal of a mouse cortical neuron. J Neurosci. 2001;21:3721–8.
51. Ahmed MS, Siegelbaum SA. Recruitment of N-Type Ca(2+) channels during LTP enhances low release efficacy of hippocampal CA1 perforant path synapses. Neuron. 2009;63:372–85.
52. Li N, Lee B, Liu RJ, Banasr M, Dwyer JM, Iwata M, et al. mTOR-dependent synapse formation underlies the rapid antidepressant effects of NMDA antagonists. Science. 2010;329:959–64.
53. Nicoll RA, Malenka RC. Expression mechanisms underlying NMDA receptor-dependent long-term potentiation. Ann N Y Acad Sci. 1999;868:515–25.
54. Carrier N, Kabbaj M. Sex differences in the antidepressant-like effects of ketamine. Neuropharmacology. 2013;70:27–34.
55. Shaffer CL, Dutra JK, Tseng WC, Weber ML, Bogart LJ, Hales K, et al. Pharmacological evaluation of clinically relevant concentrations of (2R,6R)-hydroxynorketamine. Neuropharmacology. 2019;153:73–81.
56. Ito HT, Schuman EM. Functional division of hippocampal area CA1 via modulatory gating of entorhinal cortical inputs. Hippocampus. 2012; 22:372–87.
57. Megias M, Emri Z, Freund TF, Gulyas AI. Total number and distribution of inhibitory and excitatory synapses on hippocampal CA1 pyramidal cells. Neuroscience. 2001;102:527–40.
58. Luo X, McGregor G, Irving AJ, Harvey J. Leptin induces a novel form of NMDA receptor-dependent LTP at hippocampal temporoammonic-CA1 synapses. eNeuro. 2015;2:pii: ENEURO.0007-15.2015.
59. Spruston N, Jaffe DB, Williams SH, Johnston D. Voltage- and space-clamp errors associated with the measurement of electrotonically remote synaptic events. J Neurophysiol. 1993;70:781–802.
60. Frey U, Krug M, Reymann KG, Matthies H. Anisomycin, an inhibitor of protein synthesis, blocks late phases of LTP phenomena in the hippocampal CA1 region in vitro. Brain Res. 1988;452:57–65.
61. Ho YC, Lin TB, Hsieh MC, Lai CY, Chou D, Chau YP, et al. Periaqueductal gray glutamatergic transmission governs chronic stress-induced depression. Neuropsychopharmacology. 2018;43:302–12.
62. Aleksandrova LR, Wang YT, Phillips AG. Hydroxynorketamine: implications for the NMDA receptor hypothesis of ketamine's antidepressant action. Chronic Stress. 2017;1:2470547017743511.